RESEARCH ARTICLE

Influence of cholesterol enrichment under *in vivo* and *in vitro* conditions on aggregation and deformability of erythrocytes – A comparative study

M. Kumaravel, S. P. Kasthurirangen and Megha Singh

Biomedical Engineering Division, Indian Institute of Technology, Madras 600 036, India

Aggregation and deformability of cholesterol-enriched erythrocytes obtained from hypercholesterolaemic rabbits and prepared by incubating human erythrocytes in cholesterol-enriched plasma for 2 h at 37°C are determined. The aggregation process is described in terms of parameters determined by sequentially recording and analysing the He–Ne laser light transmission data through erythrocytes suspension by a PC-AT computer-based system. The deformability of erythrocytes is determined by measuring the passage time of erythrocytes through micropores of cellulose membranes. The results show that the aggregation of human erythrocytes is enhanced due to the cholesterol enrichment process. The formed aggregates are of larger size and these sediment faster. In contrast to this, the rabbit erythrocytes do not show this phenomenon as these sediment similar to monodisperse cells. The deformability of cholesterol-enriched erythrocytes is significantly reduced.

THE phospholipids and cholesterol, constituting an integral part of the erythrocyte membrane, are exchangeable between plasma and erythrocytes[1, 2]. The equilibrium of cholesterol between plasma and erythrocytes is disrupted under certain pathological conditions as well as by artificial means. In response to a diet containing excess cholesterol fed to experimental animals, the cholesterol levels in plasma and erythrocytes are increased, resulting in the formation of spur cells and leading to haemolytic anemia[3–5]. A similar increase in these lipids in plasma and erythrocytes has been reported[6] in patients with liver cirrhosis and hyperlipaemia. The erythrocytes from hyperlipaemic rabbits fed a high-cholesterol diet show a behaviour similar to that observed in hyperlipaemic elderly patients[7].

The cholesterol enrichment of erythrocytes under *in vitro* conditions also induces morphological and rheological changes in erythrocytes, but the mechanism of these changes may be different from that under *in vivo* conditions, as the cells are incubated in cholesterol-enriched plasma for a short duration[8]. Due to the brief exposure to cholesterol-enriched plasma, the changes induced could either be due to cholesterol accumulation in the membrane or a combined effect of alteration in lipid and protein constituents of the membrane, which lead to a reduction in erythrocyte deformability[9]. This is contributed by the decrease in the mobility of the proteins[10] and morphological changes in erythrocytes[6, 11]. As the normal functioning of the erythrocyte is essential for its survival and oxygen transport in capillaries, the variation in the above parameters increases the blood viscosity, especially under low-shear flow conditions[12].

Another important parameter which changes the blood viscosity significantly is the aggregation of erythrocytes. This is a dynamic reversible process attributed to the formation of chain-like structures under stasis and slow flow conditions[13]. These structures disaggregate with increasing flow. The parameters responsible for the formation of aggregates are the negative charge of the erythrocyte membrane, the levels of fibrinogen and globulin in plasma and the applied shear force. In hypercholesterolaemia the negative surface charge contributed by the carboxyl group of sialic acid and partly by that of amino acid residues in sialoglycoproteins is decreased[14]. This reduction in sialic acid content may increase the aggregation of erythrocytes even at the same levels of fibrinogen and globulin and thus contribute in increasing the blood viscosity[15].

For determining such changes in the aggregation process a very sensitive technique is required. The techniques based on forward and backward scattering of light are found to be very sensitive for detecting these changes[16–19]. For better analysis it is essential to maintain the slow flow condition, which allows a prolonged interaction of plasma proteins and erythrocytes. This condition could be achieved by allowing the erythrocytes to sediment in plasma under the gravitational field and the associated changes could be detected by passing He–Ne laser light through the centre of the specimen chamber[20–22]. Based on this principle, we have intro-

duced a PC-AT-computer-based technique to collect data sequentially and to analyse these to present the data in terms of various aggregation parameters[23]; this technique has recently been applied to detect the changes in aggregation in blood samples of patients suffering from jaundice[24]. The objectives of the present study are to analyse by this technique the changes in aggregation of erythrocytes obtained from hypercholesterolaemic rabbits and human cholesterol-enriched erythrocytes. The deformability of erythrocytes, which plays an important role in the formation of aggregates[25], is also determined by measuring the passage time of these cells through cellulose micropore membranes. To the best of the authors' knowledge, such a study on the aggregation process of hypercholesterolaemic erythrocytes has not been reported to date.

Materials and methods

Experimental techniques

On-line He–Ne laser light erythrocyte aggregometer

This technique is based on the attenuation of laser light after passing it through the observation volume (OV) located at the centre of the specimen chamber containing erythrocytes suspension in plasma at 5% haematocrit. *Initially, the erythrocytes are monodisperse, but tend to* form aggregates, depending upon the level of plasma proteins, even during the gravitational sedimentation conditions[21]. Depending upon the size of the aggregates and erythrocytes, while passing through the OV, the transmitted light signal contains the mean intensity superimposed on the fluctuations. By sequential analysis of this signal, the aggregation process is represented in terms of the following parameters:

(a) *Aggregate size index* (ASI) – instantaneous change in the size of the aggregate, represented in terms of the number of cells.
(b) *Aggregate sedimentation time index* (ASTI) – measured as the time taken by aggregates to cross the observation volume and represented as the corresponding number of time fluctuations.
(c) *Time required for completion of process* (TRCP) – measured as the time taken for attaining the maximum intensity I_0 (as determined by plasma alone in the chamber).
(d) *Total number of fluctuations* (TNF) – observed as superimposed on the mean intensity.

For comparison of the aggregation process the data on the ASI and ASTI variation are used further to obtain the following parameters:

(a) *Effective number of cells* (ENC) present in the beam at any instant of time. This is obtained by substituting the number of cells (ΔN) responsible for the ASI variation from the corresponding number of cells N_i, and is given by

$$\Delta N = \frac{\sum_{i=1}^{4} n_i \cdot N_i}{\sum_{i=1}^{4} n_i},$$

where

n_i = number of fluctuations in the ith category of amplitude ($i = 1$–4),

N_i = average number of cells in the same category,

ENC = $N_i - \Delta N$.

(b) *Effective cellular sedimentation duration* (ECSD) is obtained from the ASTI variation as the effective time duration taken by the formed aggregates and erythrocytes to sediment through the OV, and is given by

$$\text{ECSD} = \Delta T = \frac{\sum_{i=1}^{4} n_i \cdot T_i}{\sum_{i=1}^{4} n_i},$$

where

n_i = number of fluctuations in the ith category of time ($i = 1$–4),

T_i = mean sedimentation time for the same category.

Figure 1 shows a schematic diagram of the system used for sequential analysis of the aggregation process of erythrocytes. He–Ne laser beam (power – 2 mW, Spectra Physics, USA) of wavelength 632.8 nm and diameter 1.0 mm was passed through the observation volume located at the centre of the chamber. The

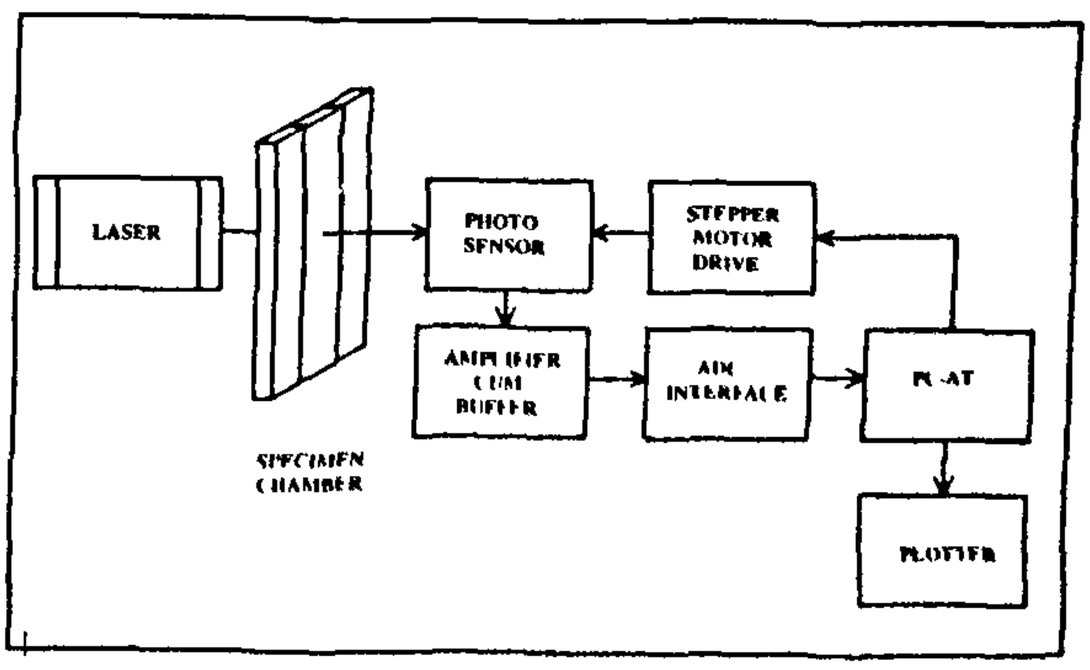

Figure 1. Schematic diagram of the system for analysis of aggregation mechanism of erythrocytes

transmitted intensity was detected by a photodiode amplifier HAD 1000A (EG&G, USA). This output was fed to a 12-bit analog-to-digital converter which was interfaced to a PC-AT.

The specimen chamber, made of optically flat glass plates, of internal dimensions 70.0 × 8.0 × 1.6 mm was filled with erythrocytes suspension in plasma at 5% haematocrit. The chamber width was kept sufficiently large to allow interaction between cells and plasma proteins for uninhibited growth of aggregates[15] and their movement away from the chamber wall[26]. Further details of computational and experimental procedure are given in ref. 23.

For analysis the system was tested with erythrocyte suspension in saline at the same concentration. No fluctuations were observed in the transmitted intensity till the completion of the process. The pattern of fluctuations in the transmitted intensity varied depending upon the concentrations of dextrans of various molecular weights in the erythrocyte suspensions[21].

Erythrocyte deformability measurement

Figure 2 shows a schematic diagram of the system used for the measurement of erythrocyte deformability. This instrument, based on initial flow rate method[27], consists of a glass syringe of 10 mm dia and 50 mm height with a constant light intensity source on one side and photodetector opposite to this, and measures the transmitted light. The detector output is interpreted as the duration elapsed to cross the observation volume and is read on the display panel of the instrument. The sample is always filled up to a level of 3.0 mm below the top of the syringe. The volume of erythrocyte suspension contained between the source and the detector is 0.6 ml. Over this height (8.5 mm) the change due to variation in the gravitational field is considered to be negligible. The lower end of the syringe is connected to a pop-top membrane holder (Nucleopore Corporation, USA) which is further connected to a three-way valve. The holder contained one disc of cellulose membrane of thickness 400 ± 25 μm consisting of curved slits of diameter 20 ± 5 μm (Grade 589, Schleicher and Schull, Germany).

These membranes for erythrocytes filtration were first introduced by Teitel *et al.*[28] as these were effective in detecting the changes in erythrocytes which pass through these slits by tank-tread motion and these were not getting blocked by white cells and other blood products[28]. In our earlier studies we have used the same membranes to detect changes in erythrocyte deformability in hypercholesterolaemia[12], myocardial infarction[29] and diabetes mellitus[22]. These observations show that the erythrocytes with reduced deformability take a longer duration to pass through the membranes and vice versa.

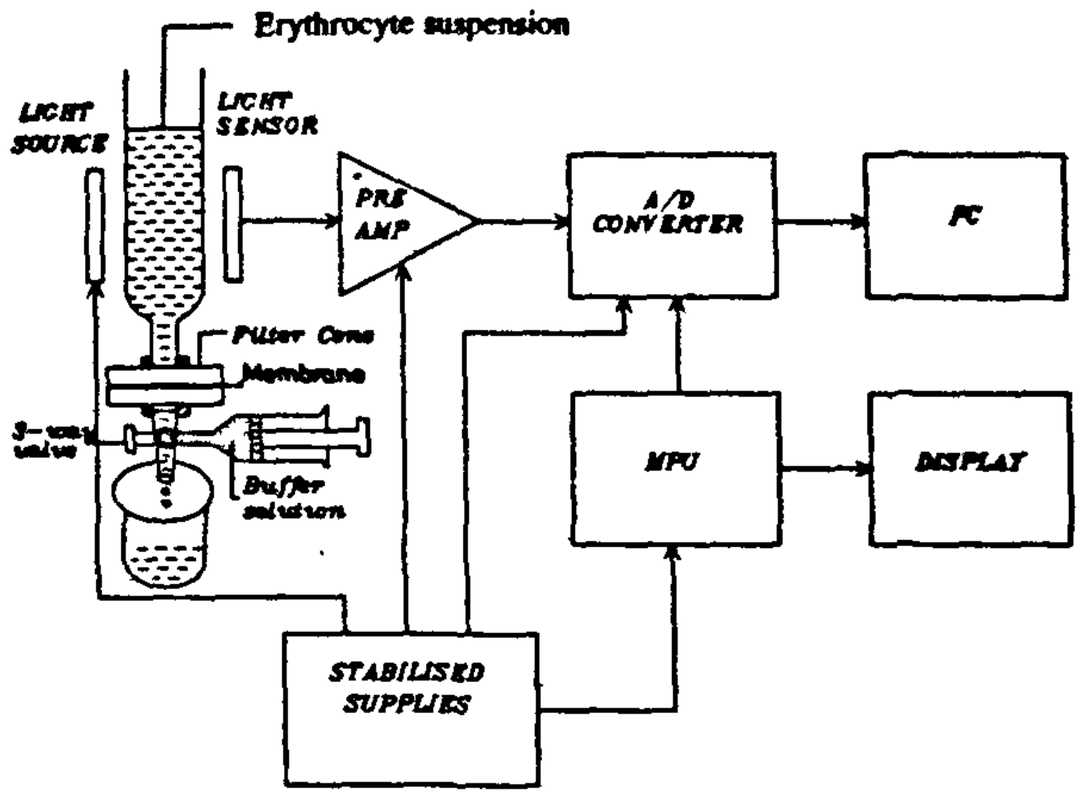

Figure 2. Schematic diagram of the system for measurement of erythrocyte deformability.

Prior to the measurement, the air bubbles trapped in the membrane and its holder were removed by flushing with a buffered saline solution from the central opening of the valve. The erythrocyte suspension was then filled up to the mark in the syringe. Due to this the transmitted light falling on the photodetector is reduced. When there is no blood sample under fully filtered condition, the amplifier output changes to maximum.

The software routine determines the number of samples N lying between these two limits, and calculates and displays the passage time (s). Two such measurements are taken with each membrane and their averaged passage time is determined. From the known volume of suspension the filtration rate (μl/s) (directly proportional to the erythrocytes' deformability) is calculated. Further details of the experimental procedure are given in ref. 12.

Sample preparations

In vivo cholesterol enrichment of erythrocytes

White albino rabbits of same age, sex and body weight (1.8–2.0 kg) were divided into two groups. Group I ($n = 6$) was fed with a normal diet (carrot, cabbage and greens) while group II ($n = 6$) was fed with a normal diet + 0.5% cholesterol per day. The lipid levels were measured regularly. After the desired cholesterol level was reached, cholesterol feeding was regulated to maintain the same level. Blood samples were collected by ear vein puncture in tubes containing citrate phosphate dextrose (CPD) (10:1.4) as an anticoagulant. Blood was centrifuged at 2000 *g* for 15 min. Plasma was separated and the buffy coat on top of the cells was removed and discarded. The cells were mixed with buff-

Table 1. Cholesterol and phospholipids in human plasma and erythrocytes before and after cholesterol enrichment

Medium	Group	Cholesterol (mg %)	Phospholipid (mg %)	C/P
Plasma	Normal	145.0 ± 8 62*	177.2 ± 8 4	0 81 ± 0 02
	CEP	248 0 ± 12 4	171.5 ± 8 5	1 45 ± 0.09
Erythrocytes	Normal	66.5 ± 7 9	67.5 ± 7 8	0 98 ± 0.01
	CEE	85.73 ± 10.2	65 2 ± 3 1	1.31 ± 0.12

*Mean ± S D.

Table 2. Cholesterol, phospholipids and C/P ratio in plasma and erythrocytes of control and cholesterol-fed (hycholest) rabbits

Medium	Group	Cholesterol (mg %)	Phospholipid (mg %)	C/P
Plasma	Control	96.3 ± 22.4*	96.5 ± 37.6	1.05 ± 0 23
	Hycholest	626.3 ± 76 8	323 0 ± 28 3	1.95 ± 0.27
Erythrocytes	Control	67.2 ± 20 5*	68.5 ± 4 07	0 97 ± 0.22
	Hycholest	170.0 ± 13 9	110 0 ± 4 08	1 53 ± 0.10

*Mean ± S.D.

ered saline (pH 7.4) and centrifuged at 2000 *g* for 10 min. The supernatant was removed. This process was repeated thrice. For measuring the aggregation of erythrocytes these cells were suspended in plasma at 5% haematocrit, whereas for deformability these were suspended in buffered saline containing 0.5% albumin to prevent their crenation[12] at 6% haematocrit.

In vitro cholesterol enrichment of erythrocytes

Fresh blood samples collected from healthy donors ($n = 12$) in test tubes containing CPD (10:1.4) were centrifuged at 2000 *g* for 10 min. The plasma was separated by aspiration. The buffy coat on top of the cells was removed and discarded.

Preparation of cholesterol-enriched plasma (CEP)

In the previously reported techniques[30, 31] to inactivate the enzyme LCAT plasma was heated to 56°C. Thus, the conversion of cholesterol to cholesterol ester was prevented. The excess of free cholesterol in plasma resulted in cholesterol enrichment of erythrocytes. In the present method[32] cholesterol was added to unheated normal plasma depending upon the availability of phospholipids in the plasma. This suspension was sonicated (Sonitron model ISM, Bombay) at a power level of 50 W at 4°C for 2 h. Thereafter, this was centrifuged at 2000 *g* for 15 min. The supernatant, cholesterol-enriched plasma, was separated and the sediment discarded.

Preparation of cholesterol-enriched erythrocytes (CEE)

Washed erythrocytes were suspended in the CEP at a haematocrit 40% and incubated for 2 h in a water bath maintained at 37°C. To obtain uniform exchange, the suspension was gently mixed at intervals of 15 min. Further details of this procedure are given in ref. 32.

After incubation, the erythrocyte suspension was centrifuged at 2000 *g* for 15 min to separate the erythrocytes and plasma. From these the suspensions for aggregation and deformability measurements were prepared by the procedures outlined above.

Lipid estimations

The erythrocyte lipids were extracted with chloroform methanol (2:1) mixture by the method of Folch *et al.*[33] and the total lipids of plasma and erythrocytes were determined by the method of Fringes *et al.*[34]

The levels of cholesterol and phospholipids of plasma and erythrocytes were determined by the methods of Baginski and Zak[35] and Naito[36], respectively.

Data collection

For collection of data on aggregation mechanism, the erythrocyte suspensions were placed between the light source and the detector. The recording of the transmitted intensity was carried out throughout the process till the observation volume was clear of aggregates, as observed

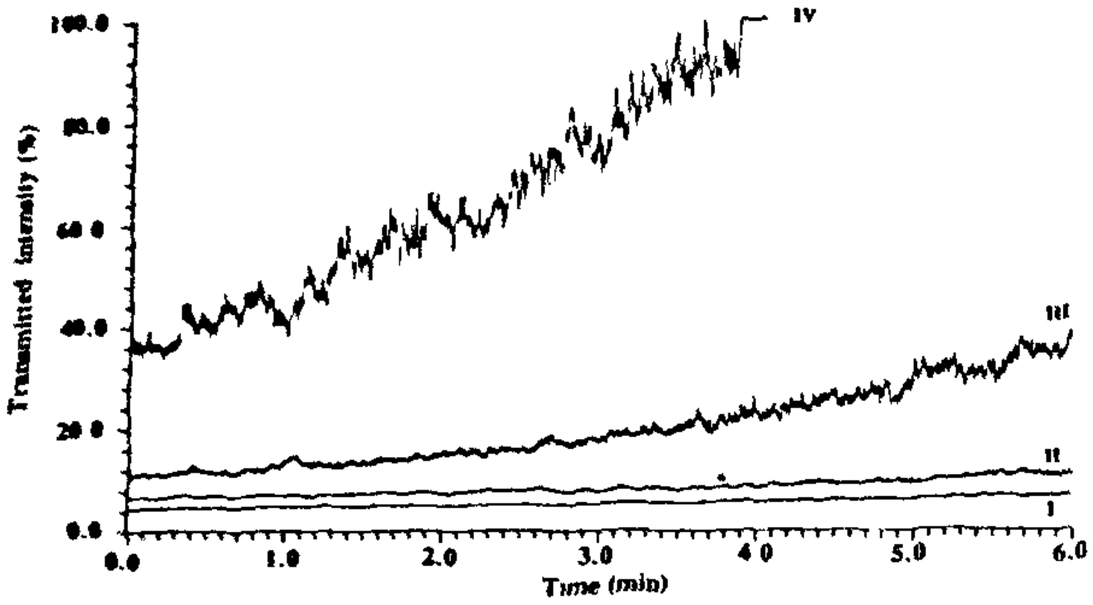

Figure 3. Variation in transmitted intensity at various time intervals of *human normal erythrocyte suspensions* at 5% haematocrit The sequential recording is presented as four segments I, II, III and IV

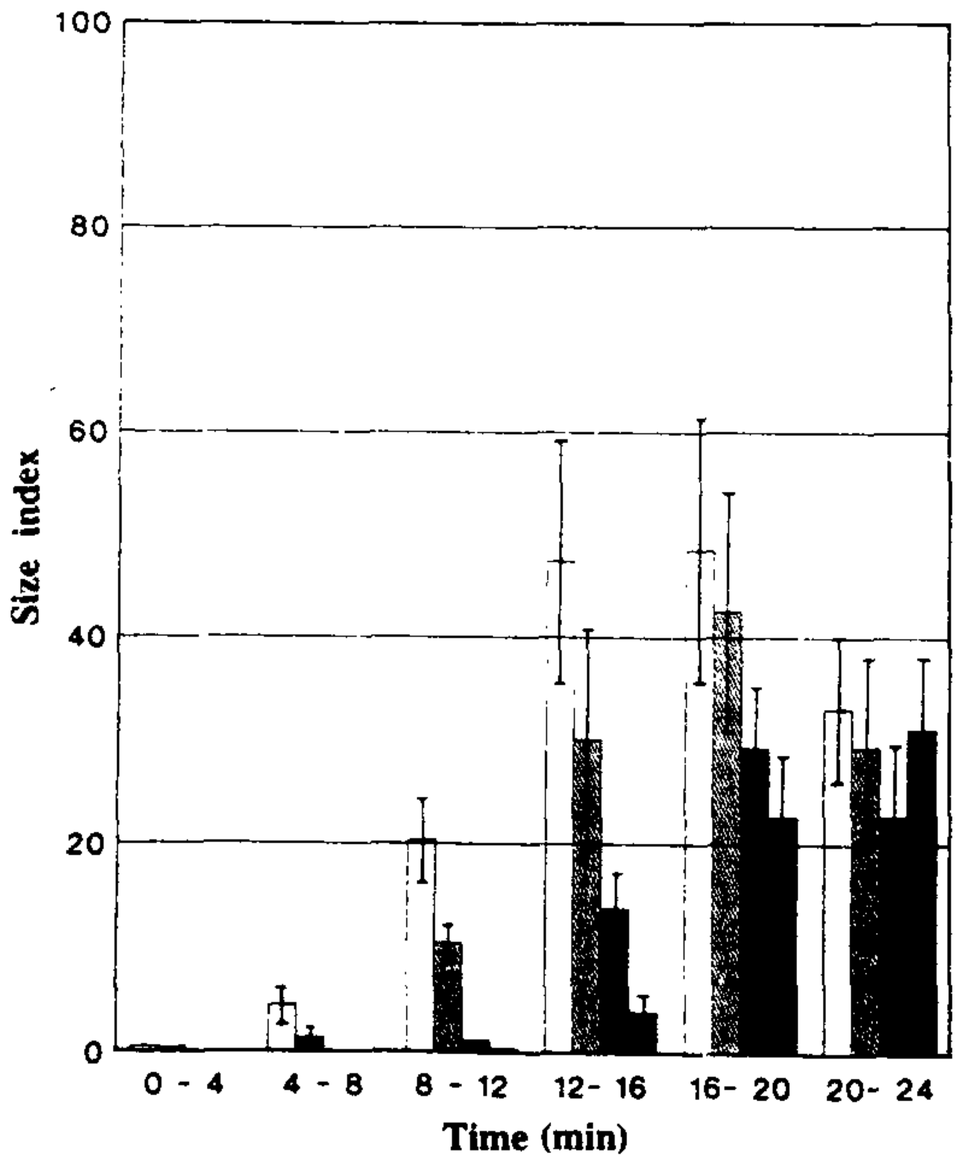

Figure 4. The variation in aggregate size index, presented as the number of fluctuations in each category at various time intervals, corresponding to the change in number of cells for normal *human erythrocyte suspension.* These categories are 3000–7000, 7000–14000, 14000–21000, 21000–29400

by the absence of fluctuation. For each set of observations a new glass chamber was used. This was a precautionary measure to avoid the artefacts caused by the sticking of various blood products on the walls of the specimen chamber.

Deformability of the control, hypercholesterolaemic and cholesterol-enriched erythrocytes was measured in terms of the first and second passage times through the cellulose membranes, as discussed above. All the samples were analysed within 2–3 h after blood collection at

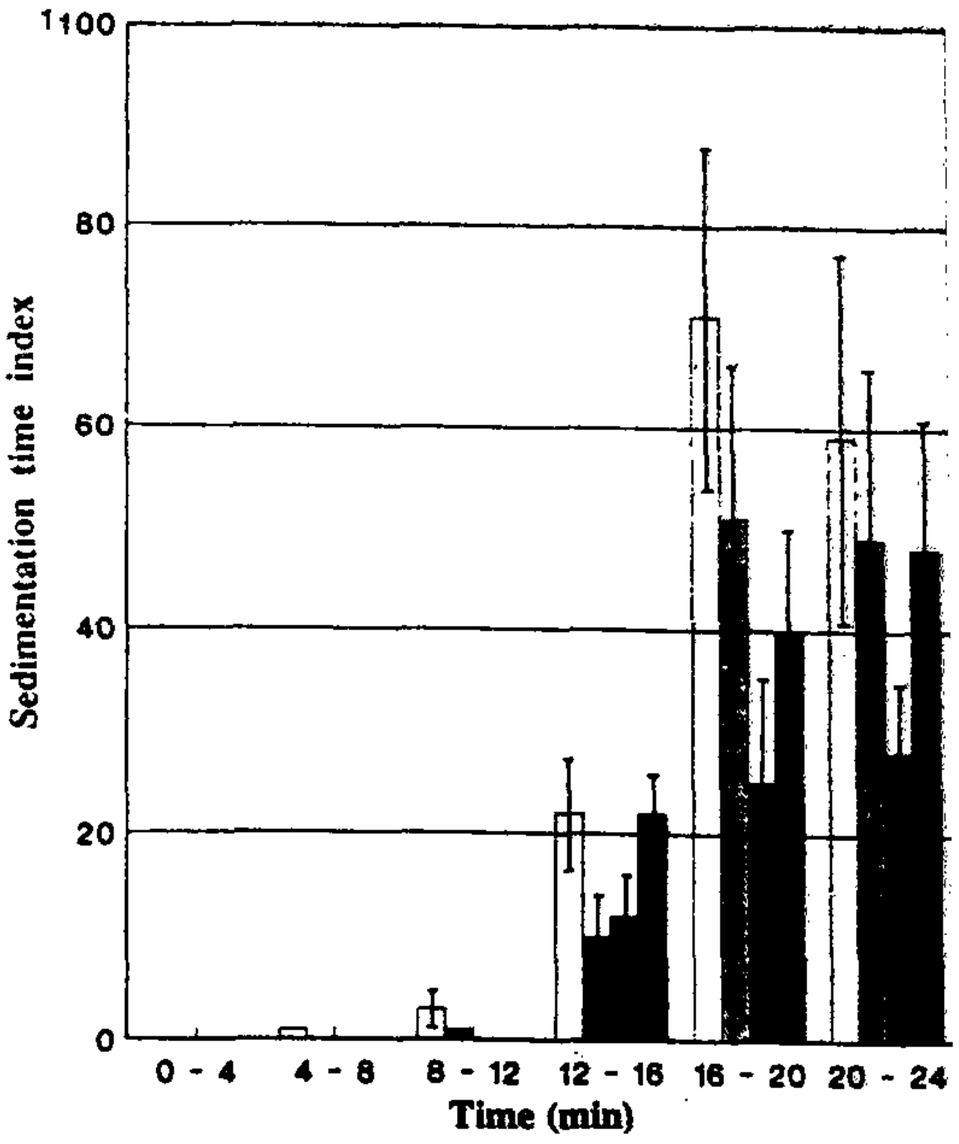

Figure 5. The variation in aggregate sedimentation time index presented as the number of fluctuations in each category corresponding to the time interval required to cross the observation volume for normal human erythrocyte suspension These categories are 0–0 15 s, 0 15–0 3 s, 0 3–0 45 s, 0 45–0 6 s

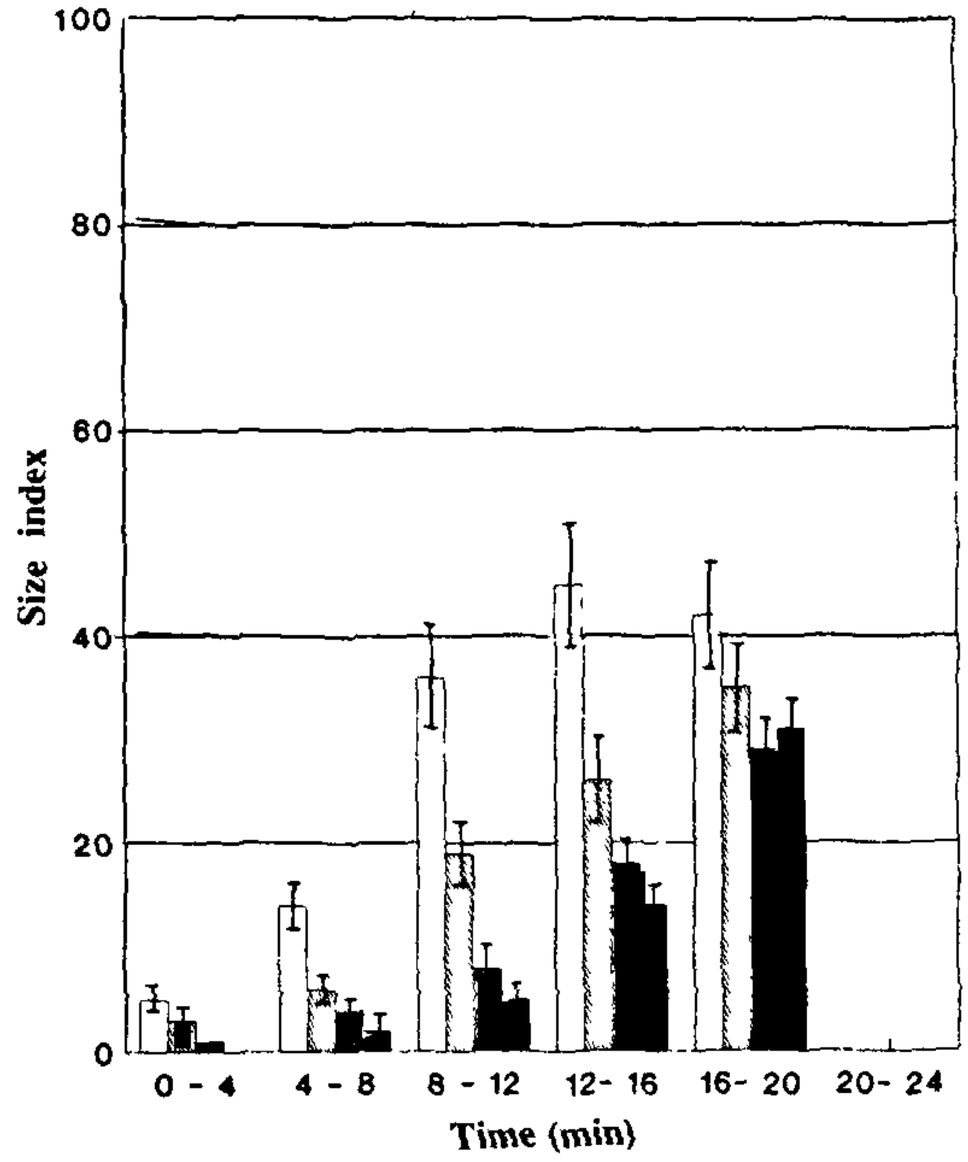

Figure 6. Variation in the aggregate size index presented as the number of fluctuations in each category at various time intervals, corresponding to the change in the number of cells for the CEE samples These categories are 3000–12000, 12000–24000, 24000–36000, 36000–48000

room temperature (25°C). The Student's *t*-test was used to compare the data for various groups.

Results

The cholesterol and phospholipids levels in plasma and erythrocytes before and after the cholesterol-enrichment process are shown in Table 1. The cholesterol content is significantly increased by adding cholesterol to this medium. The normal erythrocytes show an increase in cholesterol-to-phospholipid (*C/P*) ratio. There is no change in phospholipid composition after incubation.

Table 2 shows the levels of cholesterol and phospholipids and the C/P ratio in the plasma and erythrocytes of rabbits. Due to cholesterol feeding, the cholesterol and phospholipids levels and the C/P ratio in blood samples of these rabbits are increased.

Figure 3 shows an example of the variation of the transmitted intensity (TI) of the erythrocyte suspension of a human control sample. As evident from the figure, there are no significant fluctuations in the TI for about 5 min. Thereafter, these tend to appear in the output signal. With the increase of sedimentation duration, the amplitude of these fluctuations varies, indicating a change in aggregate size. Finally, there are no fluctuations in the TI, indicating that all the formed aggregates have crossed the observation volume in about 22 min.

Figure 4 shows the nomogram of the aggregate size index as obtained from the amplitude of the fluctuations in the erythrocyte suspensions of human control subjects. Initially, the amplitude of the fluctuations is less, which tends to increase with increasing time duration. The change in the number of cells clearly indicates that, initially, the observation volume consists of aggregates of large size, but towards the end of the process aggregates of various sizes are observed. The formation of aggregates of various sizes is further supported by the observed variation in the ASTI of a human control sample (Figure 5). The occurrence of fluctuations with a smaller time interval indicates the formation of large aggregates, which take less time to cross the observation volume.

The variation in the ASI in a suspension of the human CEE is shown in Figure 6. The pattern of the aggregate size variation is altered. The aggregation process is initiated earlier and is completed faster than for the control sample. The dominance of small-amplitude fluctuations indicates the formation of large aggregates throughout the process. Figure 7 shows the variation of the ASTI in the human CEE suspensions. Fluctuations of short time intervals are observed throughout the process, which indicate that the aggregates move faster through the OV.

Figure 8 shows a comparison of the ENC at various time intervals in the path of the laser beam. The pattern of sedimentation of the CEE is different from that of the normal human erythrocytes. The process completion time for the CEE is less than that of normal erythrocytes. Figure 9 shows the variation of the ECSD of the normal and the CEE. An increased value of this for the CEE samples shows the presence of a large number of fluctuations throughout the process compared to that of normal erythrocytes.

Two more parameters are obtained from the above figures for further comparison of the aggregation process. These are: (a) half-cells time (HCT) – required to achieve 50% of the initial number of cells in the path of the beam (from Figure 8); (b) aggregation fluctuation time (AFT) - indicating the time taken by aggregates corresponding to this HCT (from Figure 9) Table 3

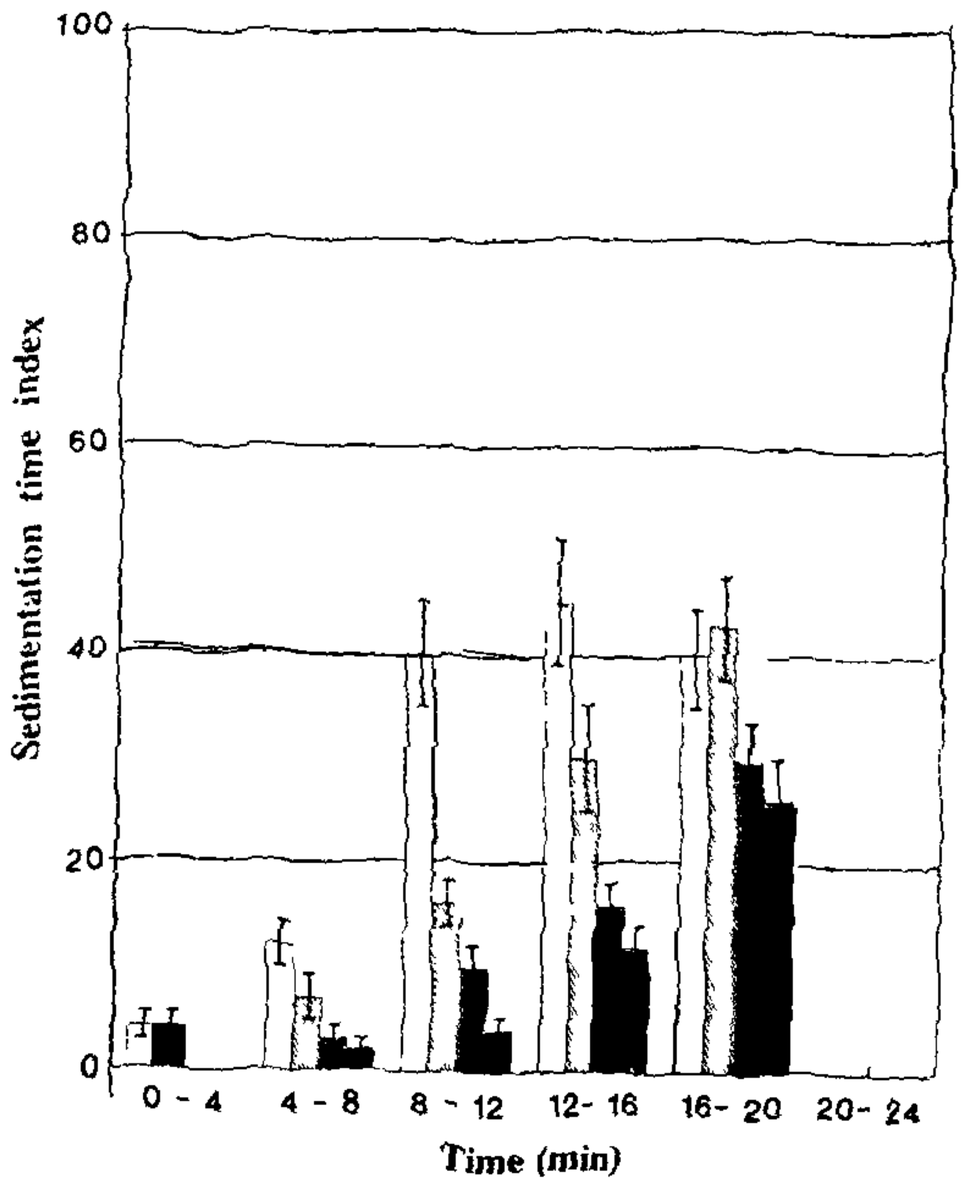

Figure 7. Aggregate sedimentation time index variation presented as the number of fluctuations in each category, corresponding to the *time intervals* required to cross the observation volume, for the CEE samples These categories are <0 375 s, 0 375–0 75 s, 0 75–1 125 s, 1 125–1 5 s

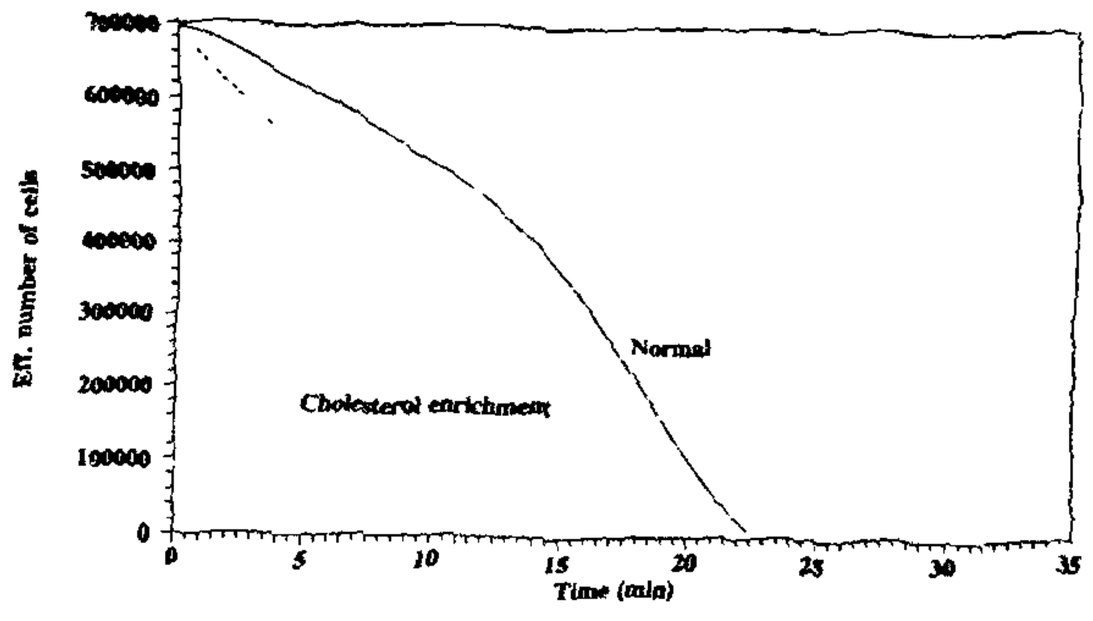

Figure 8. Variation in the effective number of cells (ENC) for the normal and the CEE samples at various time intervals

Table 3. Comparison of the aggregation parameters of human normal and cholesterol-enriched (CE) erythrocytes

	Normal	CE	p
TRCP (min)	22.4 ± 3 5*	18 5 ± 1 94	<0 025
TNF	3012 ± 467	2719 ± 281	<0 1
HCT (min)	15 9 ± 2 11	11.3 ± 1 661	<0 005
AFT (s)	0 31 ± 0 06	0 56 ± 0 103	<0 005

*Mean ± S D.

Table 4. Comparison of the aggregation parameters of erythrocytes of control and cholesterol-fed rabbits

	Erythrocytes		
Parameter	Control	Hycholest	p
TRCP (min)	277 ± 43*	232 ± 38	<0 05
ΔA_{max} (%)	4 87 ± 0 88	8 12 ± 1 13	<0 0005

*Mean ± S D.

Table 5. Comparison of the filtration time (FT) and filtration rate (FR) of erythrocytes of control and cholesterol-fed (hycholest) rabbits

	Parameter	Control	Hycholest	p
I	FT*	4 97 ± 0.87†	5.92 ± 1 04	<0.1
Pass	FR**	124 56 ± 21.63	104 34 ± 16 87	<0.1
II	FT	6.52 ± 1.13	8 13 ± 1.34	<0 05
Pass	FR	95 12 ± 17 84	75 72 ± 11.82	<0.05
Mean	FT	5 74 ± 0 99	7.03 ± 1 05	<0 05
	FR	107 79 ± 19 28	87 13 ± 11.64	<0 05

*In s.
**In μL/s.
†Mean ± S.D.

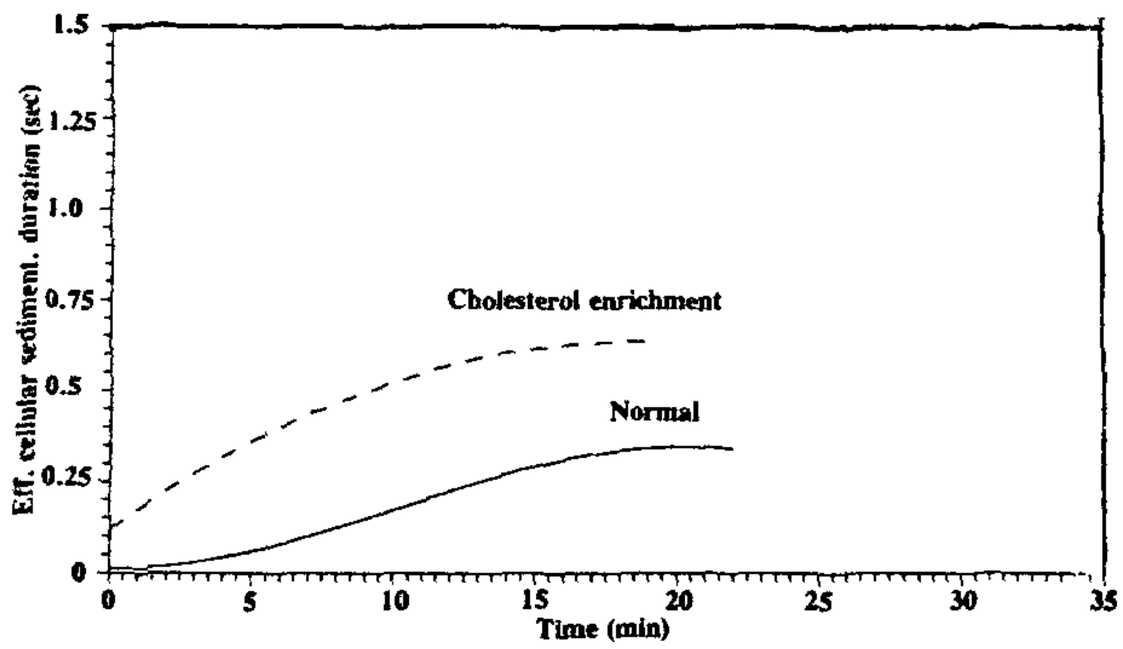

Figure 9. Variation in the effective cellular sedimentation duration (*ECSD*) *for the normal and the CEE samples* at various time intervals.

shows the variation in the above parameters along with the total number of fluctuations and the time required for completion of the aggregation process for human normal and CEE. The changes in TRCP, HCT and AFT are highly significant in the CEE compared to those of controls. This shows that the process of cholesterol enrichment alters the aggregation process of erythrocytes significantly.

In contrast to human subjects, the aggregation mechanism of rabbit erythrocytes is different. These cells do not show any significant fluctuation due to the formed aggregates. Therefore, the fluctuation amplitude (A) due to the change in transmitted intensity signal observed towards the end of the process is presented as the percentage of the maximum TI (ΔA_{max}) (%). The aggregation parameters of erythrocytes of the control compared to those of cholesterol-fed (hycholest) rabbits show significant variation (Table 4). This indicates that this process is responsible for the observed changes in the aggregation process.

The variation in passage time and filtration rate of erythrocytes of normal and cholesterol-fed rabbits is given in Table 5. The mean filtration time and filtration rate show significant variation in hypercholesterolaemic erythrocytes. The same pattern is observed in the mean values, which shows that the deformability of *in vivo*

Table 6. Comparison of the filtration time (FT) and filtration rate (FR) of human normal and cholesterol-enriched (CE) erythrocytes

	Parameter	Normal	CE	*p*
I	FT*	4 62 ± 0 43†	5.65 ± 0 53	<0 0025
Pass	FR**	131 01 ± 11.48	107 17 ± 10 85	<0 0025
II	FT	6 55 ± 0 525	8 02 ± 0 884	<0 0025
Pass	FR	92.19 ± 7 32	75 63 ± 8 42	<0 0025
Mean	FT	5 58 ± 0.38	6 83 ± 0 70	<0 0025
	FR	111.59 ± 7 44	88 76 ± 9 35	<0 0025

*In s
**In μL/s
†Mean ± S D.

cholesterol-enriched cells is decreased. By a similar process, the variation in filtration time and filtration rate of the human CEE is analysed (Table 6). The changes produced in these parameters are highly significant, indicating a decrease in erythrocyte deformability.

Discussion

The present techniques are aimed at detecting the changes in the transmitted component of light for aggregation process analysis and measurement of passage time through a cellulose membrane. The variation in parameters of the aggregation process provides details about the interaction of cellular and plasma constituents in terms of formed aggregates and their sedimentation pattern at various time intervals. Similarly, the passage time indicates the change in erythrocytes membrane structure and the interior while passing through the curved slits of the cellulose membranes. The second passage time is longer than the first one, indicating a reduced flow of erythrocytes, attributed to the presence of erythrocytes in the slits. During the second passage, these erythrocytes interact with the incoming erythrocytes, thus delaying the overall flow through the membrane. The alteration in the normal shape of erythrocytes due to the hypercholesterolaemic process[11] could partly be responsible for the observed decrease in the deformability.

The present observations show that the aggregation mechanism, as analysed by various parameters, varies significantly in *in vitro* and *in vivo* cells. Without cholesterol enrichment this directly shows a comparison between human and rabbit erythrocytes. In human cells the aggregation process, as analysed by the variation in the TI, is completed in about 22 min, whereas, under exactly identical conditions, the same process with rabbit erythrocytes suspension takes around 4 h. This variation could partly be attributed to the distribution of membrane proteins, phospholipids and fatty acids pattern of total lipids[37] and their interaction with plasma proteins. Further details of the mechanism responsible for this variation are not known. The cholesterol enrichment process is directly related to the transfer of cholesterol from plasma to erythrocytes. A significant decrease in the time required for completion of the process, the formation of large aggregates and the distribution of fluctuations indicate that the sialic acid content of the human erythrocyte membrane, which is reduced during the process[14], could partly be responsible for the enhanced tendency of aggregate formation of these cells.

The deformability of erythrocytes is significantly reduced due to the cholesterol enrichment process, which is directly attributed to the transfer of cholesterol from plasma to the erythrocyte membrane, leading to its hardening, which finally leads to discocyte–acanthocyte transformation of these erythrocytes[11]. These results are further supported by the findings of others[38–40]. Despite this change in erythrocyte deformability, the aggregation of erythrocytes is not reduced, which means these cells are still capable of adapting themselves to cell shape variation required for aggregate formation.

In conclusion, the aggregation of cholesterol-enriched erythrocytes obtained by *in vitro* (human) and *in vivo* processes is increased despite the fact that the rabbit blood does not show any distinct variation in the aggregation process over a long period compared to that of human. The erythrocyte deformability of these cholesterol-loaded cells is significantly reduced. The observed changes in human blood viscosity could be due to the aggregation and reduced deformability of the erythrocytes, whereas in rabbits this could be due to morphological changes in cells and alterations in the levels of plasma constituents.

1. Kazumuchi, K. and Ohnishi, S., *J Biochem. (Tokyo)*, 1983, **94**, 1809
2. London, I M and Schwarz, H J., *Clin Invest*, 1953, **32**, 1248
3 Ostwald, R. and Shannor, A., *Biochem J*, 1964, **91**, 146
4 Xu, D, *Shaanxi Ximyiyao*, 1983, **12**, 51
5 Shouten, J A, *Nutr Rep Int*, 1984, **29**, 1223
6 Cooper, R A, Leslie, M H, Knight, D and Detweiler, D K, *J Lipid Res.*, 1980, **21**, 1082
7 Vatsala, T. M and Singh, M, *Atherosclerosis*, 1980, **36**, 39
8 Kamber, E and Liudmila, K J, *Bioscience*, 1986, **41**, 301
9 Kanakaraj, P and Singh, M, *Indian J Biochem Biophys*, 1989, **26**, 381.

10 Kanakaraj, P., Meerarani, S and Singh, M., *Curr. Sci*, 1990, 59
11. Vatsala, T. M and Singh, M, *Biorheology*, 1980, **17**, 261.
12 Kanakaraj, P. and Singh, M., *Atherosclerosis*, 1989, **76**, 209.
13 Chien, S, Usami, S, Dellenback, R. J, Gregerson, M I., Nanninga, L. D and Guest, M M., *Science*, 1967, **157**, 829.
14 Begum, N. and Singh, M, *Indian J. Exp. Biol*, 1979, **17**, 778.
15. Chien, S, in *The Red Blood Cell* (ed Surgenor, D M), Academic Press, New York, 1975, vol. 2, pp. 1031–1133.
16 Schmid-Schönbein, H and Volger, E, *Diabetes*, 1976, **25**, 897.
17. Gaspar-Rosas, A and Thurston, G. B, *Biorheology*, 1988, **25**, 471.
18. Sowemimo-Coker, S D., Whittingstall, P., Pielsch, S, Bauersachs, R M, Wenby, B. and Meiselman, H. J, *Clin. Hemorheol*, 1989, **9**, 723.
19. Donner, M, Mills, P. and Stoltz, J. R., *Clin. Hemorheol*, 1989, **9**, 715.
20. Muralidharan, E. and Singh, M, *Clin. Hemorheol*, 1988, **8**, 715
21. Singh, M and Muralidharan, E., *Biorheology*, 1988, **25**, 237.
22. Muralidharan, E. and Singh, M, *Clin Hemorheol.*, 1991, **11**, 205.
23 Singh, M. and Kumaravel, M., *Comput. Biomed Res.*, 1994, **27**, 325
24 Kumaravel, M and Singh, M, *Clin Hemorheol*, 1994, in press.
25 Skalak, R, Zarda, P. R., Jan, K. M. and Chien, S, *Biophys J*, 1981, **35**, 771.
26. Singh, M and Vatsala, T. M, *Biorheology*, 1982, **19**, 539
27. Hanss, M, *Biorheology*, 1983, **20**, 199.
28 Teitel, P., Schmid-Schönbein, H., Gaehtgens, P and Mussler, K., Proceedings of the International Symposium on Nootropic Drugs, Mexico City, 1981, pp. 198–212.
29 Kanakaraj, P and Singh, M., *Clin Hemorheol.*, 1989, **9**, 257
30 Shiga, T., Maeda, N, Suda, T., Kon, K, Sekiya, M and Oka, S., *Biorheology*, 1979, **16**, 363
31. Deuticke, B, Grume, M, Forst, B and Leuckemeier, P., *J Memb. Biol.*, 1981, **59**, 45.
32. Singh, M. and Kanakaraj, P., *Indian J. Exp Biol*, 1985, **23**, 456.
33. Folch, J, Less, M and Stanley, G H S., *J Biol. Chem.*, 1957, **18**, 673.
34 Frings, C. S., Fendley, T W, Dunn, R. T. and Dueen, C. A, *Clin Chem.*, 1972, **18**, 673
35. Baginski, E. S. and Zak, B., in *Gradwhl's Clinical Laboratory Method and Diagnosis* (eds Frankel, S, Reitman, S. and Sommerworths, A. C), C. V. Mosby, St. Louis, 1970, p 236.
36. Naito, H K, *Clin Chem*, 1975, **21**, 1454
37. Van Deenam, L. L. M. and de Gier, J, in *The Red Blood Cell*, (ed Surgenor, D M), Academic Press, New York, 1975, vol. 2, pp. 148–211
38 Flamm, M. and Schachter, D, *Nature*, 1982, **298**, 290
39. Cooper, R A, Leslie, M H., Fischkoff, S., Shinitzky, M and Shattil, S. J., *Biochemistry*, 1978, **17**, 327.
40 Borochov, H, Abbott, R. E., Schachter, D and Shinitzky, M., *Biochemistry*, 1979, **18**, 251.

Received 9 May 1994, revised accepted 9 January 1995